ChemComm

Accepted Manuscript

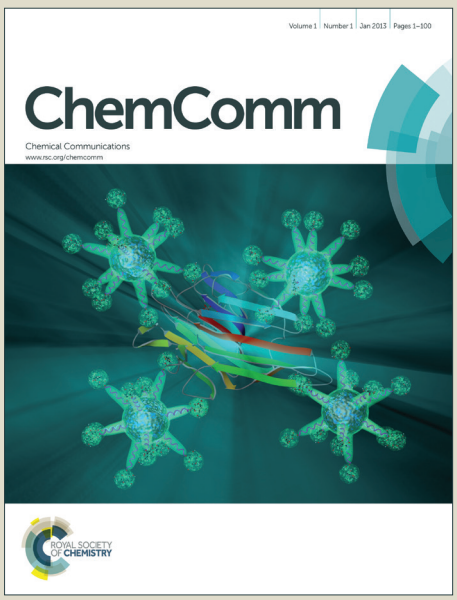

ROYAL SOCIETY OF CHEMISTRY

www.rsc.org/chemcomm

Journal Name

RSCPublishing

COMMUNICATION

The Aldimine Effect in Bis(imino)Pyridine Complexes: Non-Planar Nickel(I) Complexes of a Bis(aldimino)pyridine Ligand

Cite this: DOI: 10.1039/xoxxoooooox

Received ooth January 2012,
Accepted ooth January 2012

DOI: 10.1039/xoxxoooooox

www.rsc.org/

Blake R. Reed,[a] Sebastian A. Stoian,[b] Richard L. Lord,*[c] and Stanislav Groysman*[a]

Reduction of bis(aldimino)pyridine nickel(II) dihalide forms a non-planar bis(aldimino)pyridine nickel(I) halide. Unlike the previously reported square-planar bis(ketimino)pyridine nickel chloride, for which the spin density was localized on the ligand, the present species demonstrate Npy-Ni-X angles of 156° – 162° and a significant spin density at the metal inferred from EPR measurements and DFT calculations.

Bis(imino)pyridine [NNN] ligands are among the most commonly used ancillary ligands in transition metal chemistry and catalysis.[1-8] The success of these ligands can be attributed to their redox non-innocence (ability to accept 1-3 electrons),[5,9,10] that facilitates redox transformations at transition and main-group metal centers.[1,2,11] The large majority of the previously reported bis(imino)pyridine ligands encompass ketimine sidearms.[1-11] Specifically for nickel, several groups have recently reported that reduction of bis(ketimino)pyridine-ligated nickel(II) dihalides invariably forms square-planar nickel(II) products and a ligand-based radical anion.[10,12] Figure 1 shows three such complexes: bis(ketimino)pyridine nickel chloride (**1**), reported by Rohde and coworkers, and bis(ketimino)pyridine nickel methyl and dinitrogen complexes **2** and **3**, reported by Gambarotta and coworkers. In contrast, the chemistry of bis(aldimino)pyridines has received considerably less attention.[1,2,6,13] A recent report by Chirik and coworkers demonstrated that bis(aldimino)pyridine ligands may lead to a different chemistry than the analogous bis(ketimino)pyridine ligands.[13a] It was shown that while the reduction of bis(ketimino)pyridine complex $Fe(L^2)Br_2$ (see Figures 1 and 2 for the structures of L^1 and L^2) yields the dinitrogen complex $Fe(L^2)(N_2)_2$, the reduction of the bis(aldimino)pyridine analogue $Fe(L^1)Br_2$ eventually forms the dimeric iron compound $Fe_2(L^1)_2$.[13a] Using IR spectroscopy, the authors also showed that for the analogous $Fe(L^{1/2})(CO)_2$ complexes, the ketimine variant had a more electron-rich iron centre. Herein, we present evidence that replacing bis(ketimino)pyridine by an analogous bis(aldimino)pyridine has a significant effect on the electronic structure and reactivity of the resulting nickel complexes.

We have recently demonstrated that bidentate aldiminopyridines serve as electron storage moieties that stabilize reduced nickel centres and help activate carbon disulfide.[14] Carbon disulfide coordinated side-on, η^2 to nickel in its two-electron reduced form $[CS_2]^{2-}$. Next, we attempted one-electron oxidation to create radical character on route to C-C coupling. However, coordinated $[CS_2]^{2-}$ underwent two-electron oxidation instead. A combined spectroscopic and computational study suggested little unpaired spin density present at the metal center. We surmised that replacing bidentate iminopyridine by the tridentate bis(imino)pyridine may lead to a different electronic character of the metal center and a different coordination mode of the substrate.[15]

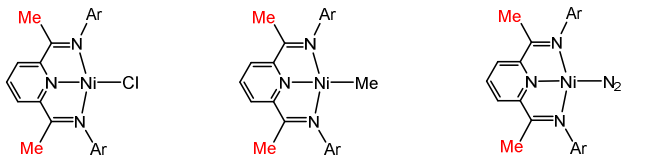

Figure 1. Top: Previously reported square planar nickel complexes of the related bis(ketimino)pyridine ligand L^2.[10,11] Ar = 2,6-diisopropylphenyl.

Our current investigation focuses on the bis(aldimino)pyridine ligand L^2 featuring bulky aryl substituents at the nitrogens (Ar = 2,6-diisopropylphenyl, Figure 2) that has been previously used with iron.[6] The ligand undergoes facile reaction with $NiCl_2$(dme) and $NiBr_2$(dme) to afford orange-red $Ni(L^2)Cl_2$ (**1**) and $Ni(L^2)Br_2$ (**2**). The

complexes were obtained as crystalline solids from THF/ether in 93 and 86% yield, respectively. Both complexes were characterized by ^{1}H NMR spectroscopy, solution magnetic moment measurements, X-ray structure determinations, and elemental analyses. ^{1}H NMR spectra demonstrate five well-resolved resonances (Figure S4 and S5) accounting for the five

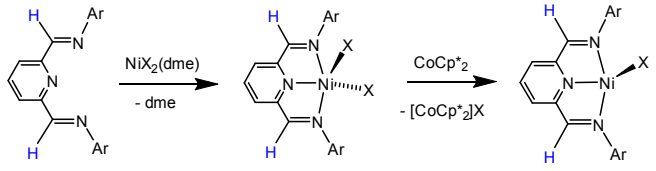

Figure 2. Synthesis of compounds 4-7 with a bis(aldimino)pyridine ligand L^1.

different protons of L^2. Solution magnetic moments are consistent with S = 1 systems (μ = 3.10 and 3.12 μB, respectively). The structures of both compounds demonstrate distorted square bipyramidal geometry at the Ni centres (see Figures S1 and S2).

Next, we investigated the one-electron reduction of **4** and **5**. The addition of $CoCp^*_2$ to the deep-orange THF solutions of **4** and **5** results in an immediate colour change to dark purple. Crystallization of the product from THF/ether yields dark purple Ni(L^1)Cl (**6**, 37%) and black Ni(L^1)Br (**7**, 48%) (Figures 2 and S3). Both compounds are related to the previously synthesized bis(ketimino)pyridine complex **1**, Ni(L^1)Cl (Figure 1) featuring Me substituents at the imino carbons. However, while Ni(L^2)Cl is planar, both Ni(L^1)Cl and Ni(L^1)Br are not. Interestingly, Ni(L^1)Br crystallizes as two different solvates (**7a** and **7b**) from the same solvent mixture (THF/ether) both having P-1 symmetry but featuring different unit cell parameters and different solvent content of the unit cell (Ni(L^1)Br•2THF for **7a** and Ni(L^1)Br•THF•OEt_2 for **7b**). Overall, **7a** and **7b** demonstrate similar structural parameters (see Figure S3 for the selected bond distances), with the major difference being N_{py}-Ni-Br angle (see below). For both **7a** and **7b** the geometry of the Ni site is non-planar. Ni centres are removed by 0.30 (**6**), 0.29 (**7a**) and 0.32 (**7b**) Å from the [NNN] planes, and the N_{py}–Ni–X angles are 162.3(1), 161.4(1), and 156.5(1)° in **6**, **7a**, and **7b**, respectively. For comparison, **1** displayed a N_{py}–Ni–Cl angle of 179°,[12] and related Cr and Co compounds with ketimino arms demonstrated N_{py}–M–Cl angles of 176 and 179°, respectively.[7,4c] Furthermore, N–C_{im} bond distances in the structures of **6**, **7a**, and **7b** appear to be slightly shorter than the respective bond distances in Ni(L^2)Cl and the related Co and Cr and complexes, which may indicate less radical character on the ligand. We also note that Chirik, Wieghardt, and coworkers reported non-planar bis(ketimino)pyridine cobalt structures for N-alkyl substituents.[9c]

Figure 4 shows the high-frequency EPR spectrum recorded at 10 K, 406.4 GHz for a ground-solid sample of **7.** Inspection of this spectrum reveals that it accounts for the presence of two nearly identical S = 1/2 species which are characterized by rhombic g tensors. Thus, while the resonances associated with the dominant component are found at g = 2.236(5), 2.144(4), and 2.048(6), those associated with the minor component are found at g = 2.263(3), 2.140(3), and 2.071(2). The frequency- and temperature-dependence of these signals are illustrated in Figures S10-12. The presence of two distinct species can be rationalized by the occurrence in the sample of a mixture of **7a** and **7b**.

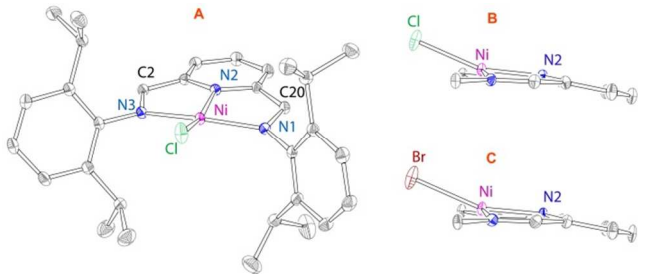

Figure 3. A: Crystal structures of 6, 50% probability ellipsoids. Hydrogen atoms omitted for clarity. B and C: side view of the cores of **6** and **7a** (aryl groups are omitted) demonstrating the non-planar distortion.

Inspection of the temperature dependent spectra suggests that both species have ground spin states consisting of isolated Kramers doublets. This observation is further confirmed by the analysis of the frequency dependence of these signals which reveals a strict linear dependence of the resonant field as function of frequency, i.e. $h\nu = g\beta H_{res}$ where h accounts for Plank's constant and β for the Bohr magneton.

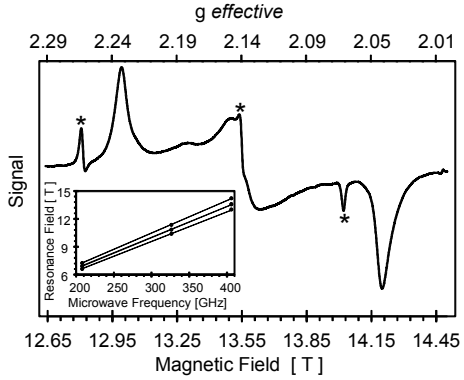

Figure 4. High-frequency EPR spectrum recorded for a ground solid sample of 7 at 10 K and 406.4 GHz. The spectrum exhibits two nearly identical S = 1/2 species. The resonances of the major component are found at g = 2.236(5), 2.144(4), and 2.048(6). The minor component resonances are labeled by (*) and are found at g = 2.263(3), 2.140(3), and 2.071(2). The inset shows the field vs. frequency dependence of the resonances of the major component.

The observed g-values are considerably larger than $g_e \approx 2.00$ expected for a radical based spin. This observation demonstrates the presence for these complexes of a ground electronic configuration for which a sizable fraction of the unpaired spin density is found localized over the metal ion. There are two distinct configurations that could account for our experimental data. Thus, we could either observe a genuine Ni(I) ion with a d^9 configuration or a high-spin Ni(II) ion for which the S = 1 spin of the nickel ion is antiferromagnetically

coupled to a $S = 1/2$ radical based spin.[16] While on the basis of the EPR spectra alone we cannot distinguish between these two possibilities, not only are the observed g values well within the range detected for other genuine Ni(I) complexes, but also our theoretical investigation, *vide infra,* supports Ni(I) character rather than Ni(II) AF-coupled to a ligand radical.[17]

To further elucidate the electronic structure of our complex, we turned to DFT calculations.[19] Consistent with our EPR data, the $S = 1/2$ state is favoured by 11.4 and 11.5 kcal/mol over the $S = 3/2$ state for Ni(L^1)Cl (**6**) and Ni(L^1)Br (**7**), respectively, and bond lengths are in agreement with the X-ray data (see Table S2). Multiple starting geometries converged to a slightly non-planar structure with N_{py}–Ni–X angles of ~177°. Care was taken to start with perpendicular N-aryl groups yet each optimized structure showed rotation by ~6 degrees. These angles differ from the X-ray structures that show a N_{py}–Ni–X angle of ~160° and rotation of the aryl groups by up to 30°. The electronic structures for **6** and **7** are best described as having a low-spin Ni^{II} centre with a radical on the bis-iminopyridine ligand, as evidenced by the spin density plots in Figure 5 and the bond length metrics in Table S2. Why, then, is there evidence for metal-centred spin density in the EPR? Could the N_{pyr}–Ni–X angle be related to this discrepancy?

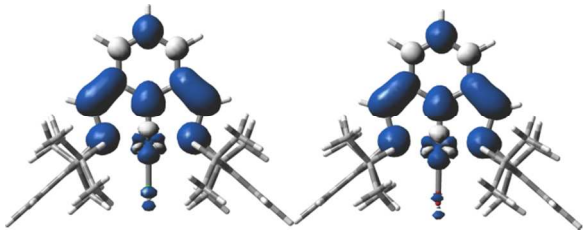

Figure 5. Spin density isosurface plots (iso = 0.002 au) for 6 (left) and 7 (right).

To answer these questions, we performed constrained optimizations varying that angle from its optimized value near linearity to a significant bend of 140° for **6** and **7**, but focus on the latter since the best EPR data was obtained for this species and the results are qualitatively similar (see Table S3 for **6** and Table S4 for **7**). This range of angles covers all of the experimentally observed N_{py}–Ni–X angles. This mode is soft with only a ~7 kcal/mol penalty for deformations up to 140°. As the angle increases there are important accompanying structural changes: (i) C_{py}–C_{im} elongates from 1.43 to 1.44 Å, (ii) C_{im}–N_{im} contracts from 1.32 to 1.31 Å, (iii) all M–L bonds elongate by 0.03–0.07 Å, and (iv) the aryl substituents on N_{im} deviate from perpendicular by up to 25°. Mulliken spin densities show an increase in the spin density at Ni from +0.06 to +0.36 and a decrease at the ligand from +0.96 to +0.79 as the angle varies from 177° to 140°. Both the ligand and metal spins are positive; one should be positive and the other negative if the antiferromagnetically-coupled Ni^{II}/L^{-} state is important. An increase in the Ni^{I} character as a function of the N_{py}–Ni–Br angle, which should lower the energy of d_{x2-y2} dramatically, is therefore not surprising and agrees well with the EPR data. The bond length changes are consistent with less ligand radical character (i and ii) and more Ni^{I} character (iii). An interesting feature of the X-ray structures of **6**, **7a** and **7b** is that the aryl group rotations are asymmetric. When combined with the finding that the N_{py}–Ni–X mode is soft (only ~2-4 kcal/mol to reach the experimental angle), these results suggest that intermolecular interactions in the crystal structures may enhance the non-planarity of this species. Thus, the electronic aldimine effect that controls the Ni oxidation state may be a consequence of the internal ligand sterics; the methyl groups in the ketimine stiffen the N_{py}–Ni–X mode due to the clash with the aryl ^{i}Pr groups based on analogous constrained optimizations on **1** and the analogue of **1** with Br (see Tables S5 and S6) where higher energies for the angle variation (up to 10 kcal/mol) and smaller rotations of the aryl groups (up to 19°) are observed.

To further investigate the differences between the non-planar bis(aldimino)pyridine complexes Ni(L^1)X (**7**) and the planar bis(ketimino)pyridine complex Ni(L^2)Cl (**1**), we investigated the reactivity of **7** with O_2. Rohde and coworkers have previously reported that the reaction of a planar **1**, featuring a ligand-based radical with O_2 led to ligand modification.[13] In contrast, **7** demonstrated metal-based reactivity with O_2. Exposure of **7** to air leads to a quick colour change to orange-brown. ^{1}H NMR spectrum of the crude reaction mixture demonstrated the presence of **4** and free ligand (Figures S10 and S11). Free ligand can be separated by the extraction of the crude reaction product with hexanes. The reaction also produced an off-white material that was not soluble in organic solvents, possibly nickel oxide. No modified ligand was observed by ^{1}H NMR spectroscopy or ESI-MS.

Conclusions

Our current investigation focused on the intriguing effect of the aldimine versus ketimine groups in the backbone of the bis(imino)pyridine complexes. We demonstrate that the one-electron reduction of the bis(aldimino)pyridine Ni(II) complexes Ni(L^2)Cl_2 and Ni(L^2)Br_2 led to the formation of non-planar tetra-coordinate complexes Ni(L^2)Cl and Ni(L^2)Br. EPR studies on Ni(L^2)Br suggest significant unpaired spin residing at the metal centre, enabling us to formulate the metal centre as Ni(I). These findings stand in contrast to the previously reported planar bis(ketimino)pyridine complexes, specifically Ni(L^1)Cl, that involved bis(ketimino)pyridine radical anion coupled with square-planar Ni(II) centre. Our computational studies delve into the origins of the observed aldimine effect on the electronic structure of the bis(imino)pyridine Ni complexes. DFT calculations reveal that while optimized geometries for both aldimine and ketimine complexes feature N_{py}–Ni–X angles of around 180°, deformation of this angle of up to 150° is not associated with a significant energy increase (~4 kcal/mol). However, this deformation does lead to the increase of the spin density on the Ni centre versus the ligand. Furthermore, we show that the ability of the aryl substituents on the imino nitrogens to rotate may be responsible for the deformation of the N_{py}–Ni–X angle thus making the aldimine

effect steric in its origin. For the aldimino species, such rotation is more facile than that for the ketimino species due to the clash of the iPr groups on the aryl rings with the Me substituents on the imino carbons.

Acknowledgements

SG acknowledges Wayne State University for start-up funding, and the NSF for current support (CHE-1349048). RLL acknowledges financial support from GVSU start-up funds. Computational resources were provided by NSF-MRI award #CHE-1039925 through the Midwest Undergraduate Computational Chemistry Consortium. Part of this work was performed at the National High Magnetic Laboratory (NHMFL) which is supported by the NSF (DMR-1157490) and the State of Florida. SAS is an NHFML Jack E. Crow postdoctoral fellow. We thank Levi A. Ekanger and Prof. M. A. Allen for fruitful discussions.

Notes and references

[a]Department of Chemistry, Wayne State University, Detroit, Michigan 48202.

[b] Department of Chemistry, Grand Valley State University, Allendale, Michigan 49401.

[c] National High Magnetic Field Laboratory, Florida State University, Tallahassee, Florida, 32310.

Electronic Supplementary Information (ESI) available: [Procedures for the synthesis of **4-7**; ORTEP diagrams of **4**, **5**, and **7a**; X-ray crystallographic details; x-ray data in cif format for **4-7(a)**; ^{1}H NMR spectra for **4** and **5**; UV-vis data for **6** and **7**, and additional computational data and details, including Cartesian coordinates for all optimized structures.]. See DOI: 10.1039/b000000x/

REFERENCES

1. For a selected review on bis(imino)pyridine ligands, see: (a) V. C. Gibson, C. Redshaw and G. A. Solan, *Chem. Rev.,* 2007, **107**, 1745.
2. For selected reviews on redox-active ligands, see: (a) P. J. Chirik and K. Wieghardt, *Science,* 2010, **327**, 794. (b) K. G. Caulton, *Eur. J. Inorg. Chem*., 2012, 435. (c) S. Enthaler, K. Junge and M. Beller, *Angew. Chem. Int. Ed.,* 2008, **47**, 3317. (d) V. Lyaskovskyy and B. de Bruin, *ACS Catal.*, 2012, **2**, 270. (e) L. A. Berben, B. de Bruin and A. F. Heyduk, *Chem. Commun*., 2014, **50**, in press. (e) Q. Knijnenburg, S. Gambarotta and P H. M. Budzelaar, *Dalton Trans*., 2006, 5442.
3. (a) B. L. Small and M. J. Brookhart, *Am. Chem. Soc.*, 1998, **120**, 7143.(b) B. L. Small, M. Brookhart and A. M. A. Bennett, *J. Am. Chem. Soc*., 1998, **120**, 4049.
4. (a) G. J. P. Britovsek, V. C. Gibson, B. S. Kimberley, P. J. Maddox, S. J. McTavish, G. A. Solan, A. J. P. White and D. J. Williams, *Chem. Commun*., **1998**, 849. (b) G. J. P. Britovsek, M. Bruce, V. C. Gibson, B. S. Kimberley, P. J. Maddox, S. Mastroianni, S. J. McTavish, C. Redshaw, G. A. Solan, S. Strömberg, A. J. P. White and D. J. Williams, *J. Am. Chem. Soc.*, 1999, **121**, 8728.
5. B. De Bruin, E. Bill, E. Bothe, T. Weyhermüller and K. Wieghardt, *Inorg. Chem*. 2000, **39**, 2936.
6. (a) T. K. Lane, M. H. Nguyen, B. R. D'Souza, N. A. Spahn and J. Louie, *Chem. Commun*., 2013, **49**, 7735. (b) T. K. Lane, B. R. D'Souza and J. Louie, *J. Org. Chem*., 2012, **77**, 7555. (c) B. R. D'Souza, T. K. Lane and J. Louie, *Org. Lett*., 2011, **13**, 2936.
7. (a) I. Vidyaratne, J. Scott, S. Gambarotta and R. Duchateau, *Organometallics* 2007, **26**, 3201. (b) J. Scott, I. Vidyaratne, I. Korobkov, S. Gambarotta and P. H. M. Budzelaar, *Inorg. Chem*., 2008, **47**, 896. (c) I. Vidyaratne, I. Scott, S. Gambarotta, P. H. M. Budzelaar, *Inorg. Chem*. 2007, **46**, 7040.
8. For selected examples, see: (a) C. C. H. Atienza, C. Milsmann, S. Semproni, Z. R. Turner and P. J. Chirik, *Inorg. Chem*., 2013, **52**, 5403. (b) J. M. Darmon, Z. R. Turner, E. Lobkovsky and P. J. Chirik, *Organometallics*, 2012, **31**, 2275. (c) K. T. Sylvester and P. J. Chirik, *J. Am. Chem. Soc.,* 2009, **131**, 8772.
9. (a) A. M. Tondreau, S. C. E. Stieber, C. Milsmann, E. Lobkovsky, Th. Weyhermüller, S. Semproni and P. J. Chirik, *Inorg. Chem.,* 2013, **52**, 635. (b) A. M. Tondreau, C. Milsmann, E. Lobkovsky and P. J. Chirik, *Inorg. Chem*. 2011, **50**, 9888. (c) A. C. Bowman, C. Milsmann, E. Bill, E. Lobkovsky, T. Weyhermüller, K. Wieghardt and P. J. Chirik, *Inorg. Chem*., 2010, **49**, 6110. (d) A. C. Bowman, C. Milsmann, C. C. H. Atienza, E. Lobkovsky, K. Wieghardt and P. J. Chirik, *J. Am. Chem. Soc.* 2010, **132**, 1676. (e) B. M. Wile, R. J. Trovitch, S. C. Bart, A. M. Tondreau, E. Lobkovsky, C. Milsmann, E. Bill, K. Wieghardt and P. J. Chirik, *Inorg. Chem*., 2009, **48**, 4190. (f) S. C. Bart, E. Lobkovsky, E. Bill, K. Weighardt and P. J. Chirik, *Inorg. Chem.,* 2007, **46**, 7055. (g) S. Ch. E. Stieber, C. Milsmann, J. M. Hoyt, Z. R. Turner, K. D. Finkelstein, K. Wieghardt, S. DeBeer and P. J. Chirik, *Inorg. Chem.,* 2012, **51**, 3770.
10. D. Zhu, I. Thapa, I. Korobkov, S. Gambarotta and P. H. M. Budzelaar, *Inorg. Chem*., 2011, **50**, 9879.
11. For selected recent examples of main group compounds ligated by redox-active bis(imino)pyridines, see: (a) T. W. Myers and L. A. Berben, *Chem. Sci*., 2014, **5**, 4771. (b) T. W. Myers and L. A. Berben, *Chem. Commun*. 2013, **49**, 4175. (c) J. Scott, S Gambarotta, I. Korobkov, Q. Knijnenburg, B. de Bruin and P. H. M. Budzelaar, *J. Am. Chem. Soc.,* 2005, **127,** 17204.
12. T. D. Manuel and J.-U. Rohde, *J. Am. Chem. Soc.,* 2009, **131**, 15582–15583.
13. (a) S. K. Russell, C. Milsmann, E. Lobkovsky, T. Weyhermuller and P. J. Chirik, *Inorg. Chem*., 2011, **50**, 3159. (b) F. Morale, R. W. Date, D. Guillon, D. W. Bruce, R. L. Finn, C. Wilson, A. J. Blake, M. Schroder and B. Donnio, *Chem. Eur. J*., 2003, **9**, 2484. (c) D. Gong, B. Wang, H. Cai, X. Zhang and L. Jiang, *J. Organomet. Chem*., 2011, **696**, 1584.
14. (a) A. Bheemaraju, J. W. Beattie, R. L. Lord, P. D. Martin and S. Groysman, *Chem. Commun.,* 2012, **48**, 9595. (b) A. Bheemaraju, J. W. Beattie, E. G. Tabasan, P. D. Martin, R. L. Lord and S. Groysman, *Organometallics*, 2013, **32**, 2952.
15. (a) Y.-E. Kim, J. Kim and Y. Lee, *Chem. Commun*. 2014, **50**, 11458. (b) S. Chakraborty, J. Zhang, J. A. Krause and H. Guan, *J. Am. Chem. Soc.* 2010, **132**, 8872.. (c) F. Huang, C. Zhang, J. Jiang, Z. - X. Wang and H. Guan, *Inorg. Chem*., 2011, **50**, 3816.
16. For this case we expect the g tensor of the (SNi = 1; SLigand = 1/2)St = 1/2 ground state to be essentially determined by the nickel site, i.e. .($\mathbf{g}_t = \frac{4}{3}\mathbf{g}_{Ni} - \frac{1}{3}\mathbf{g}_{Ligand}$ where g_{ligand} ≈ 2.00)
17. (a) V. V. Saraev, P. B. Karaikivskii, I. Svodoba, A. S. Kuzakov, and R. F. Jordan, *J. Phys. Chem. A*., 2008, **112**, 12449. (b) T. C. Harrop, M. M. Olmstead and P. K. Mascharak, *J. Am. Chem. Soc*., 2004, **126,** 14714. (c) C. Uyeda and J. C., Peters, *Chem. Sci*., 2013, **4**, 157. (d) G. Bai, P. Wei, A. K. Das and D. W. Stephan, *Dalton Trans*., 2006, 1141. (e) G. Pilloni, A. Toffoletti, G. Bandoli, and B. Longato, *Inorg. Chem*., 2006, **45**, 10321. (f) J. Telser, Y.-C. Horng, D. F. Becker, B. M. Hoffman and S. W. Ragsdale, *J. Am. Chem. Soc*., 2000, **112**, 182.
18. L. Hermosilla, G. J. M. de la Vega, C. Sieiro and P. Calle, *J. Chem. Theory Comput*. 2011, **7**, 169.
19. B3LYP/ 6-311G(d,p). See SI for full details.

